Figure 9. AES depth profile of Nicalon SiC fibers that have been dip-coated in ~0.1 M (2% w/w) solution of $(CH_3)_2S\cdot BHBr_2$ and pyrolyzed under NH_3 to 1000 °C. Ar^+ sputtering rate = 125 Å/min.

700–1000 Å for these coatings. BN coatings formed from higher concentrations of precursor usually resulted in the formation of BN aggregates interbridging between fibers.

SiC (Nicalon). Coated single fibers (18% w/w solution) were examined in a procedure similar to that described above. Again, evidence of a coating of BN is clearly visible in the SEM (Figure 7b). In addition, several areas containing BN aggregates are also apparent. The Auger spectrum of a BN coated SiC fiber is shown in Figure 8. Analysis of the surface showed the presence of B and N and an additional smaller peak for C. Ar^+ ion sputtering to 1000 Å gave the expected B and N peaks and addi-

tionally Si (92 eV) and O (510 eV) peaks indicative of slight penetration into the fiber core. Coating of SiC fiber bundles was accomplished by dip-coating a fiber bundle in 2% w/w solutions of $(CH_3)_2S\cdot BHBr_2$ in CH_2Cl_2. The resulting fibers were examined by SEM, which indicated a thin coating of BN at the surface. A depth profile study (Figure 9) indicated a coatings of approximately 250 Å.

In summary, the $(CH_3)_2S\cdot BHBr_2/NH_3$ system offers a simple method for the preparation of boron nitride ceramics that has a number of unique advantages over either conventional CVD routes or known chemical precursors for the formation of boron nitride coatings. Thus, as demonstrated by the results discussed above, BN coatings of 125–2500 Å can be readily formed on either Al_2O_3/ZrO_2 or SiC fibers by varying the concentrations of the coating solutions. Preliminary work has demonstrated similar coating on smooth Sumitomo alumina fibers. Furthermore, with this method turbostratic boron nitride having oxidative stability to at least 820 °C in air may be produced by precursor pyrolyses carried out as low as 650 °C. We are currently exploring applications of this precursor and other III–V Lewis acid–base complexes for the formation of III–V ceramic coatings on a variety of substrates.

Defect Formation in Ag(I)–, Pb(II)–, Sn(II)–, and Bi(III)–β″-Aluminas

G. S. Rohrer and G. C. Farrington*

Department of Materials Science and Engineering, University of Pennsylvania, 3231 Walnut St., Philadelphia, Pennsylvania 19104

Received March 13, 1989

Ion exchange can be used to synthesize many mono-, di-, and trivalent isomorphs of the well-known fast ionic conductor Na(I)–β″-alumina, among them the Ag(I)–, Sn(II)–, Pb(II)–, and Na(I)–Bi(III) forms. These four compositions normally are colorless and electronically insulating, but they become purple semiconductors when heated to approximately 650 °C in a low partial pressure of oxygen. They are very hygroscopic, and coloration occurs only if samples have been partially hydrated prior to the high-temperature treatment but not if they are first dried carefully at elevated temperature in a dry oxygen atmosphere. The optical absorption arises from metal clusters formed during the dehydration process in the conduction layers. In single crystals, the coloration reaction is reversible and no bulk decomposition can be detected. However, powdered samples of Pb(II)–β″-alumina treated at 650 °C in 15% H_2/85% N_2 have been shown to decompose into a mixture of lead metal and other products of the partial decomposition of β″-alumina. The results underscore the great sensitivity of the various β″-aluminas to hydration, a phenomenon that must be considered in any careful study of the structures and properties of these materials.

Introduction

Na(I)–β″-alumina, a well-known fast ionic conductor of Na(I) ions, has the general formula, $Na_{1+x}Mg_xAl_{11-x}O_{17}$, where x is about 0.67. The rapid cation diffusivity in this compound makes it possible to replace its entire Na(I) content with a wide variety of mono-, di-, and trivalent cations by relatively simple ion-exchange reaction.[1,2] This

remarkable ion-exchange chemistry provides a route to the synthesis of many unusual materials, some of which have been shown to have potential applications as solid electrolytes[3] and solid-state lasers.[4]

The optical and electrical properties of several β″-alumina isomorphs have been found to change during heating

(1) Farrington, G. C.; Briant, J. *Fast Ion Transport in Solids*; Vashishta, P., Mundy, J. N., Shenoy, G. K., Eds.; North Holland: Amsterdam, 1977; p 395.

(2) Sattar, S.; Ghosal, B.; Underwood, M. L.; Mertwoy, H.; Saltzberg, M. A.; Frydrych, W. S.; Rohrer, G. S.; Farrington, G. C. *J. Solid State Chem.* **1986**, *65*, 231.

(3) Cole, T. *Science*, **1983**, *221*, 915.

(4) Farrington, G. C.; Dunn, B.; Thomas, J. O. *Cryst. Lattice Defects Amorphous Mater.* **1985**, *12*, 915.

in vacuum.[2] For example, when Eu(III)–β″-alumina is heated in a vacuum, its fluorescence shifts from red to greenish yellow, indicating that Eu(III) ions have been reduced to the Eu(II) state.[5] In addition, when Pb(II)–β″-alumina is treated similarly, color centers form and it becomes semiconducting.[6] These reactions clearly demonstrate that electronic defects can form in the β″-aluminas and dramatically affect their physical properties.

These electronic defects are not well understood. The reduction of Eu(III)–β″-alumina has been examined by several authors who proposed that oxygen ions might be lost from the structure and the cations reduced to preserve charge neutrality.[5,7,8] A similar mechanism was proposed to account for defect formation in Pb(II)–β″-alumina.[6] It must be pointed out that none of the previous investigations demonstrated the loss of structural oxygen experimentally. In fact, in the case of Pb(II)–β″-alumina, experiments guided by this hypothesis yielded irreproducible results, which indicated that other, as-yet unidentified factors might be reponsible for the reaction.[6]

It has been known for some time that the properties of various monovalent β″-aluminas isomorphs are water-sensitive.[9,10] Although the hydration of monovalent β″-aluminas has been studied extensively, much less has been known about the hydration of the divalent and trivalent isomorphs.[11] Recent investigations in this laboratory have shown that the divalent β″-aluminas react readily with water.[12] The fact that these materials are extremely hygroscopic led us to consider the role of water in the coloring reaction. The results presented here demonstrate that water is, in fact, central to the reaction and the key factor previously unrecognized.

This paper presents the results of an investigation of color center formation in Ag(I)–, Pb(II)–, Sn(II)–, and Bi(III)-β″-alumina. The goals were to identify the reaction responsible for defect formation and to examine its effect on the other physical characteristics of these materials. This paper describes the results of thermal analysis, ac impedance spectroscopy, optical absorption, and electron spin resonance experiments. In addition, X-ray powder diffraction was used to study the decomposition of Pb-(II)–β″-alumina exposed to atmospheres containing hydrogen.

Experimental Procedures

Single crystals of Na–β″-alumina were grown by the flux evaporation method.[13] The crystals were then doped with ^{22}Na, a radiochemical label used to determine the extent of subsequent ion-exchange reactions. Ion exchange was considered complete when samples showed the expected weight change and no residual ^{22}Na could be detected. In the case of partial exchanges, the extent of ion exchange was determined from the change in the ^{22}Na activity in the samples. The details of the ion-exchange reactions are given below.

Ag(I) exchanges were carried out in molten AgNO$_3$ at 280 °C in a covered crucible in air. Generally, two reactions in fresh salt, each of about 4-h duration, produced crystals that were fully

exchanged. Other Ag(I) exchanges, carried out at 350 °C, were complete after 5 h. The exchanged crystals were clear, colorless, and crack-free.

Pb(II) exchanges were carried out in molten PbCl$_2$ at 500–550 °C in sealed, evacuated quartz ampules. Generally, three or four reactions in fresh salt, each about 45 min, produced crystals that were fully exchanged. Exchanges carried out in air produced colorless crystals, and exchanges carried out in evacuated ampules resulted in colored crystals.

Sn(II) exchanges were carried ouut in molten anhydrous SnCl$_2$ at 400 °C. The molten exchange salt was contained in an alumina boat, and the reactions were performed in a dry, inert atmosphere. Generally, two reactions in fresh salt, each of about 20 min, produced crystals that were fully exchanged. With Sn(II), exposure to the exchange salt was as short as feasible, because longer exposures degraded the crystals.

Bi(III) exchanges were carried out in sealed, evacuated, quartz ampules with BiI$_3$ at 440–480 °C for 20 h. Usually, only about one-third of the sodium was replaced by Bi(III) during such treatment. Although greater levels of exchange were obtained by annealing the crystals and repeating the process, full exchange was never achieved. In the best case, about 75% of the sodium was replaced by using this method.

Some of the fully exchanged single-crystal samples were crushed to prepare powders for the thermogravimetry (TG) measurements. The crystals were sieved to select particles between 40 and 150 μm. Samples used for the TG–EGA measurements weighed 40–90 mg. All thermal gravimetry experiments were made with a Du Pont 951 TG microbalance controlled by a Model 990 thermal analyzer. A V-G Micromass PC mass spectrometer system equipped with a silica capillary inlet attachment was used to analyze the gases evolved from the sample in the TG cell. This mass spectrometer system continuously measured the partial pressures of O$_2$, H$_2$O, CO$_2$, N$_2$, and Ar over the sample during the dehydration process. Gases for the TG experiments were flowed at the rate of 150 cm^3/min. "Wet" gases were obtained by bubbling gas through distilled water, and "dried" gases were obtained by passing gas over CaSO$_4$.

The sieved powders were hydrated in the following way. First, a sample was heated at 500–550 °C to constant weight in the TG cell. This was considered the dry weight. The sample was then cooled to room temperature at 0.5 °C/min in flowing wet gas, during which its weight typically increased by about 2% of the total dry weight. Finally, portions of the samples were decomposed in the TG cell at 10 °C/min in a flowing inert gas to analyze the gases evolved. Since the compositions of the anhydrous compounds are well-known, it is a simple matter to calculate the composition with respect to hydration by assuming the the entire weight change is due to hydration or dehydration.

Colored crystals of Ag(I)–, Sn(II)–, Bi(III)–, and Pb(II)–β″-alumina were produced in three ways. The first was by vacuum annealing in which the crystals were sealed in evacuated quartz ampules and heated. Typically, a crystal was heated at 650 °C for 24 h in a residual gas pressure of about 8 μmHg. The sample was then quenched to room temperature either by removing it from the furnace and placing it directly on a cool surface or by immersing it in cool water. The second method for coloring crystals involved heating them in flowing purified argon. The argon was first purified by passing it over CaSO$_4$ and then over copper turnings at 485 °C. The flowing gas method had the advantage that a sample could be treated in a variety of gases without changing the sample temperature. In the third method, crystals were heated in flowing forming gas (15% H$_2$/85% N$_2$). The conductivity and optical absorption data presented here were obtained with crystals that were vacuum annealed.

Ac impedance spectroscopy was used to measure the electrical conductivity of single crystals of Pb(II)–, Ag(I)–, and Bi(III)/Na(I)–β″-alumina. Single crystals were cut into rectangular slabs with approximate dimensions of 0.2 × 0.3 × 0.025 cm. Blocking gold electrodes were sputtered onto two opposing faces of each crystal perpendicular to the conduction layers. For measurements above room temperature, silver paint was applied on top of the gold to ensure good contact to the platinum electrodes of the spring-loaded conductivity cell. For low-temperature measurements, platinum wires were attached to the gold-coated faces with silver paint. Low-temperature measurements were made in an

(5) Ghosal, B.; Mangle, E. A.; Topp, M. R.; Dunn, B.; Farrington, G. C. *Solid State Ionics* **1983**, *9, 10*, 273.

(6) Rohrer, G. S.; Farrington, G. C. *Solid State Ionics* **1988**, *28–30*, 1142.

(7) Carrillo-Cabrera, W.; Thomas, J. O.; Farrington, G. C. *Solid State Ionics* **1986**, *18, 19*, 645.

(8) Saltzberg, M. A.; Thomas, J. O.; Wappling, R. *Solid State Ionics* **1988**, *28–30*, 1563.

(9) Garbarczyk, J.; Jakubowski, W.; Wasiucionek, M. *Solid State Ionics* **1983**, *9, 10*, 249.

(10) Dudney, N. J.; Bates, J. B. *J. Am. Ceram. Soc.* **1987**, *70*, 816.

(11) Garbarczyk, J.; Jakubowski, W.; Wasiucionek, M. *Solid State Ionics* **1986** *18, 19*, 653.

(12) Rohrer, G. S.; Farrington, G. C. *Mater. Res. Bull.* **1988**, *23*, 1747.

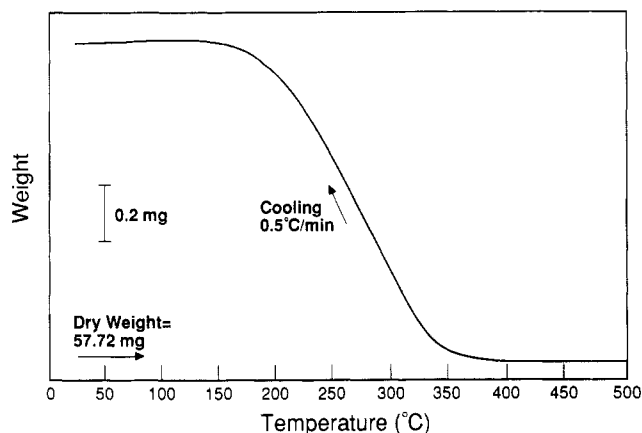(13) DeNuzzio, J. Ph.D. Thesis, University of Pennsylvania, 1986.

Figure 1. Thermogram showing hydration of Pb(II)–β''-alumina upon slow cooling in a wet gas.

Oxford Instruments liquid nitrogen cryostat. Pure, dried argon was flowed over the sample during each measurement. Impedance data were collected with an automated temperature control and impedance measurement system consisting of a Hewlett-Packard 4192A LF impedance analyzer, a Solartron 1250 frequency response analyzer, and a Micristar temperature controller, all of which were controlled by a Hewlett-Packard 9000 computer. At each temperature, the impedance was measured from 1×10^{-3} to 1.3×10^{7} Hz. The electronic and ionic conductivities were separated by using the complex impedance method. Since ionically blocking electrodes were used, no ionic conductivity should have occurred at low frequencies. Therefore, the constant, low-frequency, phaseless component of the conductivity was taken to be the electronic component.

Optical absorption measurements were made either with a Cary 14 spectrophotometer or a Perkin-Elmer Lambda 4C spectrophotometer. Low temperature measurements were made using an Oxford Instruments liquid nitrogen cryostat. The optical absorption measurements were made parallel to the c axis of the crystalline platelets, which were typically 0.1–1.0 mm thick along the c axis. The electron spin resonance spectra of the colored crystals were also studied from 2.5 K to room temperature by using a homodyne-type spectrometer. X-ray powder diffraction measurements were made by using an automated sealed tube Rigaku powder diffractometer operating at 50 kV and 40 mA. Finely ground samples were dispersed on a glass sample holder for the powder diffraction measurements. The patterns were measured from 5 to 70° in 2θ, using Cu Kα radiation.

Results

Thermal Analysis. Figure 1 shows the thermogram for the hydration of Pb(II)–β''-alumina. The sample increased in weight during cooling in wet nitrogen from 350 to 150 °C at 0.5 °C/min. The total weight gain was 1.9%, which indicates that the final composition was Pb(II)$_{0.83}$Mg$_{0.67}$Al$_{10.33}$O$_{17}$·(H$_2$O)$_{0.78}$. This composition is comparable to that of other samples studied. In each case, nearly one H$_2$O per Pb(II) cation was absorbed. Figure 2 shows the thermogram for the dehydration reaction in the TG cell. The weight loss occurred in two steps between 200 and 400 °C which indicates that water is bound at two different sites or by two different mechanisms in Pb(II)–β''-alumina. Of the isoimorphs considered in this paper, this is the only one that exhibited this behavior. The mass spectrometer indicated two increases in the partial pressure of water vapor over the sample that were simultaneous with the two weight losses (see Figure 3). The partial pressures of the other four gases monitored during the experiment (including O$_2$) remained constant throughout the experiment. From this we have concluded that the weight gain during cooling in the wet gas and the weight loss observed during heating in the dry gas were due to the intercalation and deintercalation of water, re-
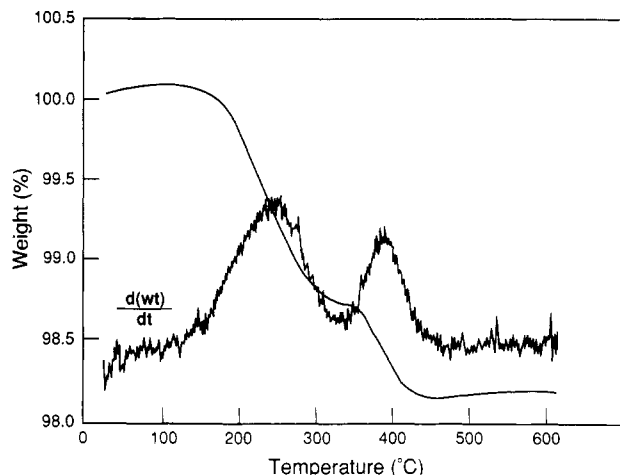

Figure 2. Thermogram for the thermal decomposition of hydrated Pb(II)–β''-alumina. Two weight losses can be observed.
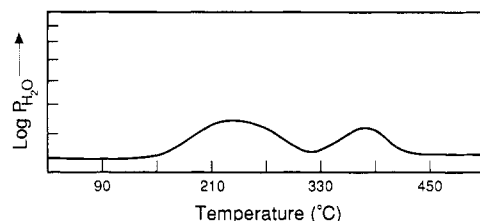

Figure 3. Partial pressure of water over Pb(II)–β''-alumina measured simultaneously with the TG data in Figure 2. These data verify that water is evolved from the sample. The units on the ordinate are arbitrary.

spectively. Similar experiments were performed on Sn-(II)–, Ag(I)–, and Bi(III)–Na(I)–β''-alumina. The results show that each of these compounds react with water in a similar way to form hydrated compounds.

Several additional thermal analysis experiments designed to explore more completely the conditions under which Pb(II)–β''-alumina hydrates were performed. In the first, a fine powder of Pb(II)–β''-alumina was heated isothermally in the TG cell at 150 °C for 16 h in P$_2$O$_5$-dried air flowing at the rate of 150 cm^3/min. After this treatment, the sample composition was Pb$_{0.83}$Mg$_{0.67}$Al$_{10.33}$O$_{17}$·(H$_2$O)$_{0.20}$. This result demonstrates that Pb(II)–β''-alumina is an extremely good desiccant. In fact, at this temperature we were not able to prevent powdered samples from absorbing water from flowing gases, no matter how the gases were dried. Larger single crystals, such as those used in ionic conductivity experiments, also absorbed water. A single crystal of Pb(II)–β''-alumina, 0.86 × 0.5 × 0.09 cm, was heated in humid air at 150 °C for 14 days. By measurement of the weight loss during dehydration, it was found that it had reached the composition Pb$_{0.83}$Mg$_{0.67}$-Al$_{10.33}$O$_{17}$·(H$_2$O)$_{0.27}$. It should also be noted that, because of the very small surface to bulk ratio of the monocrystal, the dehydration kinetics were very slow. At 550 °C, 90 min was required to remove all of the water from the crystal. It is therefore clear that large single crystals can retain bulk water for over an hour at 550 °C, even though this is well above the dehydration temperature.

It was also found that Pb(II)–β''-alumina powder also hydrates at room temperature. An anhydrous crystal was crushed and sieved so that the particle size ranged from 40 to 150 μm. The powder was then exposed to normal laboratory air at room temperature for 7 days and then dehydrated in the TG. From the weight loss on heating, the composition was found to be Pb$_{0.83}$Mg$_{0.67}$Al$_{10.33}$O$_{17}$·(H$_2$O)$_{0.21}$. It is reasonable to conclude that any small
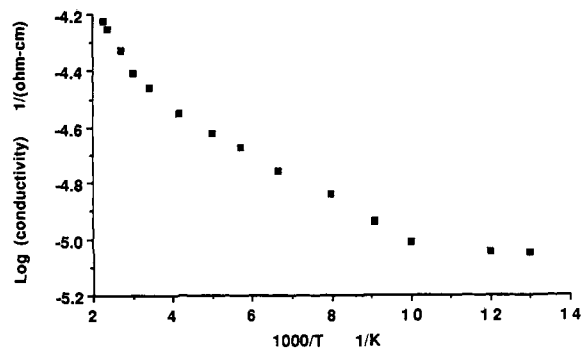
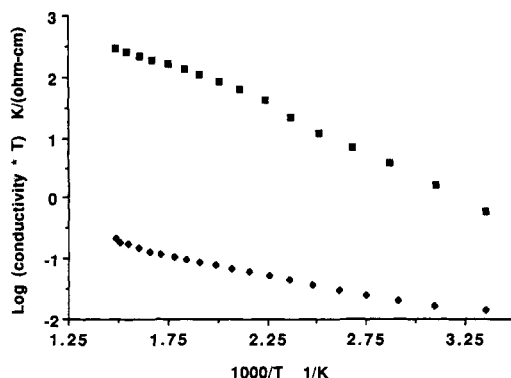**Figure 4.** Low-temperature dc electronic conductivity of colored Pb(II)-β″-alumina.

Figure 5. Arrhenius-type plot showing the ionic (■) and electron (◆) conductivities of Pb(II)-β″-alumina above room temperature.

Figure 6. Comparison of the electron conductivities of three colored β″-alumina isomorphs: (■) Bi(III)$_{0.28}$–Na(I)$_{0.84}$–β″-alumina; (◆) Ag(I)-β″-alumina; (▲) Pb(II)-β″-alumina.

Figure 7. Optical absorption spectrum of colored Pb(II)-β″-alumina: (top) room temperature and (bottom) liquid nitrogen temperature. This sample was colored by heating for 24 h at 720 °C in a vacuum.

sample, such as a crystal for X-ray diffraction analysis, if exposed to room air will partially hydrate.

Electronic Conductivity. Figure 4 shows the low-temperature variation of the electronic conductivity of a sample of Pb(II)-β″-alumina that had been vacuum annealed for 8 h at 650 °C in a quartz tube with a residual gas pressure of 8 μmHg. The dc conductivity of the sample was ohmic. The conductivity increased with increasing temperature, but the log σ versus $1/T$ plot is not linear. The activation energy for conduction is very small and increased continuously with temperature. Although the conductivities of different samples varied greatly (the highest at room temperature being approximately 5×10^{-3} (Ω cm)$^{-1}$) the form of the temperature dependence was similar from sample to sample. Figure 5 compares the electronic and ionic conductivities of Pb(II)-β″-alumina. The electronic component of the conductivity is clearly much lower than the ionic component and has a lower activation energy.

Figure 6 shows the electronic conductivities of three different isomorphs between room temperature and 400 °C. These data were obtained in dried, purified argon to avoid bleaching the samples. In the Bi(III)/Na(I) sample, 50% of the Na(I) was exchanged by Bi(III). This sample was colored as the result of being synthesized in an evacuated tube. The Ag(I)-β″-alumina and the Pb(II)-β″-alumina were colored by heating in a vacuum at 650 °C. Although the activation energy for conduction increases with increasing temperature, Ahrrenian behavior can be approximated over a small range of temperature. For example, if we arbitrarily choose the high-temperature region of the data, the activation energy for conduction in Ag(I)-β″-alumina is the highest at 0.45 eV, followed by Pb(II)-β″-alumina at 0.13 eV, and then Bi(III)/Na(I)-β″-alumina at 0.08 eV.

Electron Spin Resonance Spectroscopy. The only unpaired spins detected in the ESR spectra of Pb(II)-,
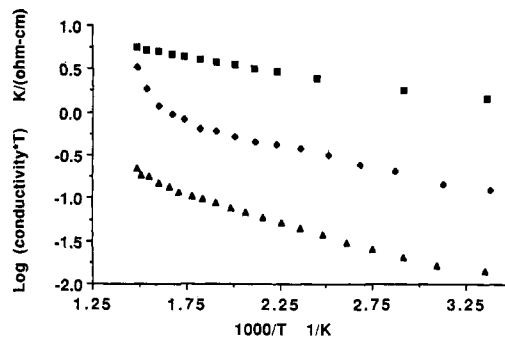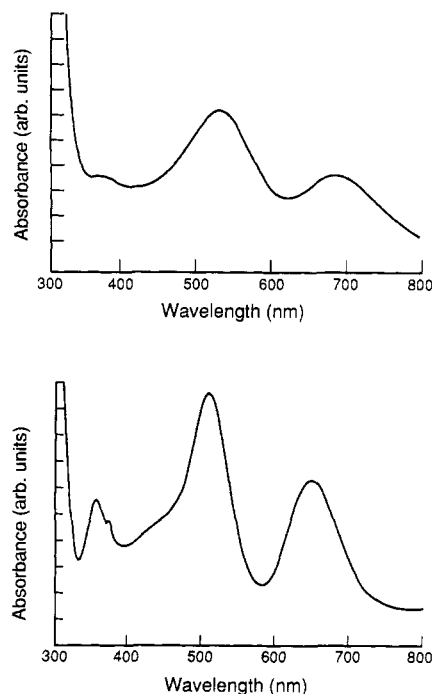
Ag(I)-, and Bi(III) Na(I)-β″-alumina were assigned to Mn(II). Manganese is a substitutional impurity for magnesium, the stabilizing ion in the spinel block of the β″-alumina crystals. The concentration of spins was in the ppm range relative to magnesium. These substitutional point defects were detected in both colored and bleached samples of the three isomorphs studied. Since no other unpaired spins were detected, it appears that only diamagnetic defects exist in the colored crystals.

Optical Absorption Spectroscopy. Figures 7-10 show the room-temperature optical absorption of colored Pb-(II)-, Sn(II)-, Bi(III) Na(I)-, and Ag(I)-β″-alumina. The absorption spectrum of Pb(II)-β″-alumina at liquid nitrogen temperature is shown for comparison (see Figure 7, bottom). Crystals colored by annealing in vacuum, purified argon, and forming gas were examined. The peak positions and relative intensities were the same, regardless of the coloring method or the amount of color introduced in the crystal. The temperature dependence of the optical absorption bands in Pb(II)-β″-alumina was also studied. As the temperature was decreased, the bands narrowed and shifted to the blue, which indicates that they arise from isolated centers coupled to the lattice. The broad
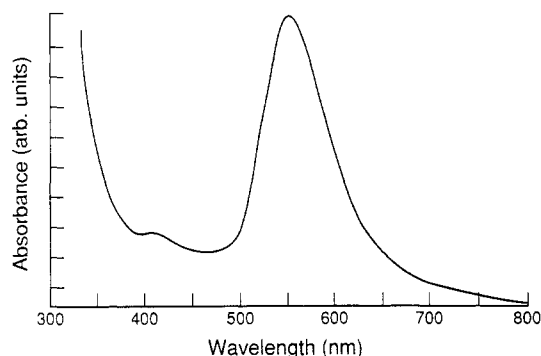
Figure 8. Optical absorption spectrum of colored Sn(II)–β''-alumina at room temperature. This crystal was heated at 700 °C for 90 min in a vacuum.
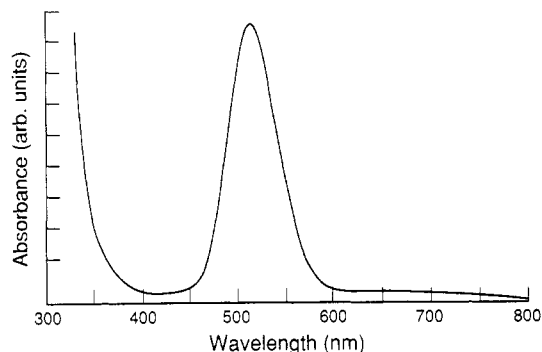

Figure 9. Optical absorption spectrum of colored Bi(III)–Na(I)–β''-alumina at room temperature. This crystal was colored during synthesis, which was performed in a vacuum.
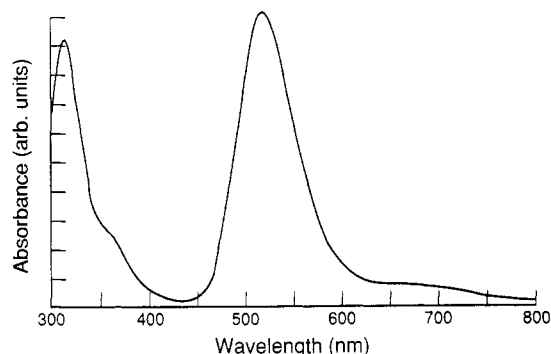

Figure 10. Optical absorption spectrum of colored Ag(I)–β''-alumina at room temperature. This crystal was heated at 650 °C for 8 h in a vacuum.

optical absorptions make the crystals appear purple when viewed in transmitted light; deeply colored crystals can appear opaque.

Discussion

The section first presents a discussion of the relationship of hydration to color center formation in β''-alumina and proposes a mechanism for the coloration reaction. Then the spectroscopic data and the possible defect species that may exist in the colored compounds are discussed. Finally, the decomposition of Pb(II)–β''-alumina is considered.

Coloration Reaction. The coloration reaction is reversible; the color can be bleached from a sample by heating it an atmosphere containing oxygen. The temperatures required for coloring and bleaching were found to vary somewhat from isomorph to isomorph. At 650 °C, 30–60 min was required to color or bleach a single crystal of Pb(II)–β''-alumina 3 × 2 × 0.5 mm in size. The coloration process proceeded from the edges of the crystal perpendicular to the conduction planes. Similarly, when

a sample was bleached, the colorless areas grew from the edges. These observations indicate that the transport of some species, a reducing agent, or a defect center occurs along the conduction planes during the coloring/bleaching processes. Since color spreads across several millimeters of crystal in less than 1 h at 650 °C, the defects involved are very mobile.

The thermal analysis results described in the preceding section clearly demonstrate that the various β''-aluminas studied in this investigation hydrate. To test whether water is essential for the coloring reaction, a single crystal of Pb(II)–β''-alumina was first heated in flowing, dried oxygen at 650 °C for 3.5 h. Previous thermal analysis data have shown that a sample treated in this manner should be anhydrous. The gas supply was then changed to argon that had been passed over copper turnings at 485 °C to remove any residual oxygen. The crystal remained colorless. The crystal was then partially hydrated by cooling it slowly in humid oxygen from 330 to 100 °C, and then it was reheated to 650 °C in the purified argon. This time the crystal colored. These reactions could be repeated and demonstrate that well-dried crystals do not color in purified argon, though partially hydrated crystals do. We also observed that all crystals, regardless of their pretreatment, color at 650 °C in a mixture of 15% H_2/85% n_2 (forming gas).

On the basis of these observations, we propose that, when a crystal of partially hydrated Pb(II)–, Sn(II)–, Ag(I)–, or Na(I)–Bi(III)–β''-alumina is heated in a vacuum or in purified argon, water begins to diffuse out of the bulk of the crystal, exiting through the faces perpendicular to the conduction planes. Some of the water then reduces conduction layer cations at the crystal–vacuum interface. The protons produced presumably bond to structural oxygens forming hydroxyl-like groups to maintain charge neutrality. The reduced conduction layer cations absorb light in the visible range and color the sample. The identity of these reduced species, which form at the surfaces of the crystal, will be discussed below. When samples are heated in forming gas, gaseous hydrogen can reduce conduction layer cations directly, so water need not be present for the reaction to proceed. In support of this model, we have observed that the coloring process is single crystals takes approximately the same amount of time as the dehydration process. It is also interesting to note that coloring during vacuum dehydration is quite common among transition-metal zeolites and occurs by a mechanism similar to that proposed here.[14,15]

An alternate explanation for the coloring reaction is that it is the result of the loss of oxygen ions from the structure, presumably oxygens in or near the conduction planes. If this were the case, the coloration should occur whenever the partial pressure of oxygen in the surrounding atmosphere is sufficiently low, regardless of whether or not water is present. The partial pressure of oxygen in the experiment above was fixed, and the crystal colored only when it was partially hydrated. This indicates that dehydration is the key to the reaction, not structural oxygen loss.

Possible Defect Species in the Colored β''-Alumina Isomorphs. The reaction just proposed suggests that reduced cation defect species should exist in the conduction layers. Table I lists possible defect species that might be formed in such a reduction reaction. Nearly all of these

(14) Gellens, L. R.; Mortier, W. J.; Schoonheydt, R. A.; Uytterhoeven, J. B. *J. Phys. Chem.* **1981**, *85*, 2783.

(15) Beyer, H.; Jacobs, P. A.; Uytterhoeven, J. B. *J. Chem. Soc., Faraday Trans. 1* **1976**, *72*, 674.

defects have already been observed in other solids. By comparing our spectroscopic data with data from other sources, it was possible to determine the defects most likely present in the colored crystals.

The ESR silence excludes the presence of several reduced cation species (Pb(I), Bi(II), Ag(0)), colloidal metal particles, and single electrons in oxygen ion vacancies (F⁺ centers). The defects that remain fall into three categories. First are diamagnetic, monoatomic, reduced cations such as Pb(0) in Pb(II)–β″-alumina, Sn(0) in Sn(II)–β″-alumina, and Bi(I) in Bi(III)–Na(I)–β″-alumina. Second are diamagnetic F centers—two electrons trapped at an oxygen ion vacancy. In the final group are dimers and other small molecular species formed from the reduced cations. Although paramagnetic defects cannot be ruled out for colored Sn(II)–β″-alumina, because ESR measurements were not made on this compound, it can be shown that they would not account effectively for the optical results.

The optical absorption spectra are useful to limit further the possible defect species present in the colored crystal. For example, it is unlikely that the observed spectra arise from any of the diamagnetic, monoatomic, reduced cation species mentioned above. The optical absorptions of Bi(I), Pb(0), and Sn(0) isolated in alkali-metal halides have been reported.[16-18] In no case do the absorption band(s) assigned to these species match all the bands observed in the colored β″-alumina isomorphs. Although some of the bands are similar, the principal elements of the spectra cannot be explained by absorption from these species. The presence of Sn(I) is not excluded by the ESR experiments, but the optical absorption of this ion cannot account for the absorption bands in colored Sn(II)–β″-alumina.[19] Therefore, the possibility that Bi(I), Pb(0), Sn(0), or Sn(I) accounts for the observed spectra can be ruled out on the basis of the optical data.

Furthermore, the absorptions in the colored β″-aluminas are unlikely to be produced by F centers. Paramagnetic F⁺ centers would generally coexist with F centers. Their absence does not in itself exclude the existence of F centers but, together with the position of the absorption bands, makes it doubtful for the following reason. Both F⁺ and F centers are observed in α-alumina; the absorption bands assigned to the F⁺ center are at 230 and 259 nm, while the absorption band for the two-electron F center is at a higher energy, 204 nm.[20] In Na(I)–β-alumina, the absorption band assigned to the F⁺ center is at 300 nm.[21] If an F band existed, it would presumably occur at a shorter wavelength. Because of the structural similarity of β- and β″-alumina, the F and F⁺ bands should occur at similar energies. Thus, the absorption band(s) in the colored β″-aluminas, which occur at wavelengths much larger than 300 nm, cannot be assigned to F centers. It should be pointed out that the same is true for hydroxyl and hydroxide impurities that might form as the result of heating in hydrogen or vacuum dehydration.[22]

On the other hand, the absorption spectra of the colored crystals are quite similar to those reported for dimers or small molecules of the metal atoms that might be present. The optical absorption of dilead Pb₂, has been observed at 10 K in an argon matrix.[23] The positions of the absorption bands in colored Pb(II)–β″-alumina at 77 K are close, though slightly red-shifted, to those reported for Pb₂. The relative intensities of the bands in colored Pb(II)–β″-alumina are also similar to those observed for the matrix-isolated Pb₂. The absorption spectrum of Sn₂ has also been studied in a low-temperature inert matrix.[24] A strong band was observed at 500 nm and a weaker band at 600 nm. The room-temperature absorption spectrum of colored Sn(II)–β″-alumina showed a strong band at 550 nm, which overlapped a weaker band in the 650-nm region of the spectrum. Bi₂ has also been studied in rare-gas matrices at 10 K.[25,26] A strong band at 513 nm that overlapped a weaker band at 565 nm was observed in absorption experiments.[25] Weak bands at lower energies have been assigned to Bi₄ molecules.[26] Absorptions were present in colored Bi(III)–Na(I)–β″-alumina at room temperature near these positions, and the strongest band was centered at 513 nm.

The strongest absorpton band in the spectra of these diatomic molecules is due to the molecular X to A transition. Because of comparable bonding configurations, the separation of these energy levels is similar in each of these dimers. Thus, the principal absorption band assigned to the transition occurs at about the same wavelength, 500 nm. In each of the colored β″-aluminas, the strongest absorption band is also centered near 500 nm. In each case, the observed spectra are similar to those reported previously for the dimers. For this reason, it appears likely that the absorptions in the colored β″-aluminas are caused by diatomic molecular species. Since the present observations were made at higher temperatures than those reported previously, there is a red-shift in the band positions. Host lattice effects may also contribute to some of the differences. The spectral data for the three β″-alumina isomorphs, for the diatomic molecules, and for selected monoatomic species are summarized in Tables II–IV.

It might appear that Ag(I)–β″-alumina is an exception to this model, since the absorption spectrum of colored Ag(I)–β″-alumina is not similar to the absorption spectrum of the Ag₂ molecule.[27] However, because Ag(I)–β″-alumina has twice the cation density of the other β″-alumina isomorphs, it is reasonable to expect larger aggregates to form. For example, optical absorptions in vacuum dehydrated Ag–zeolite A have been assigned to the Ag_6^{n+} cluster.[14] The color center absorptions in vacuum-dehydrated Ag–zeolite A assigned to the Ag_6^{n+} clustered occurred at 513 and 364 nm. The positions of these bands agree very closely with those observed in vacuum-dehydrated Ag(I)–β″-alumina. Therefore, the absorptions in Ag(I)–β″-alumina are most likely to be the result of similar aggregates. The optical absorption data relevant to Ag(I)–β″-alumina are summarized in Table V.

In summary, we used our ESR and optical absorption data to make the following tentative assignments. The visible absorption bands observed in Pb(II)–, Sn(II)–, and Bi(III)–Na(I)–β″-alumina are due to metal dimers, and the absorption bands in Ag(I)–β″-alumina are likely to be the result of larger aggregates, such as Ag_6^{n+}. It appears that these defect species are formed as the result of the vacuum

(16) Radhakrishna, S.; Srinivasa Setty, R. S. *Phys. Rev. B.* **1976**, *14*, 969.

(17) Dalal, M. L.; Sivaraman, S.; Murti, V. Y. G. S. *Phys. Status Solidi B* **1985**, *132*, 591.

(18) Egemberdiev, Zh.; Seeman, V.; Zazubovich, S.; Jaanson, N. *Phys. Status Solidi B* **1979**, *92*, 335.

(19) Delbecq, C. J.; Hartford, R.; Schoemaker, D.; Yuster, P. H. *Phys. Rev.* **1976**, *13*, 3631.

(20) Crawford, J. H., Jr. *Semicond. Insul.* **1983**, *5*, 599.

(21) O'Donnell, K.; Barklie, R. C.; Henderson, B. *J. Phys. C: Solid State Phys.* **1978**, *11*, 3871.

(22) Schulman, J. H.; Compton, W. D. *Color Centers in Solids*; Pergamon Press: New York, 1962; pp 163–168.

(23) Teichman, R. A., III; Nixon, E. R. *J. Mol. Spectrosc.* **1976**, *59*, 299.

(24) Epting, M. A.; McKensie, M. T., Jr.; Nixon, E. R. *J. Chem. Phys.* **1980**, *73*, 134.

(25) Teichman, R. A., III; Nixon, E. R. *J. Chem. Phys.* **1977**, *67*, 2470.

(26) Bondybey, V. E.; Schwartz, G. P.; Griffiths, J. E.; English, J. H. *Chem. Phys. Lett.* **1980**, *76*, 30.

(27) Ozin, G. A.; Huber, H. *Inorg. Chem.* **1978**, *17*, 155.

Table I. Possible Reduced Defect Species

	Isomorph			
defect type	Pb(II)	Sn(II)	Bi(III)	Ag(I)
monoatomic paramagnetic	Pb(I)	Sn(I)	Bi(II) Bi(0)	Ag(0)
monoatomic diamagnetic	Pb(0)	Sn(0)	Bi(I)	–
vacancy paramagnetic	$V_0^{\bullet}$	$V_0^{\bullet}$	$V_0^{\bullet}$	$V_0^{\bullet}$
vacancy diamagnetic	$V_0^{\bullet\bullet}$, V_0^{x}	$V_0^{\bullet\bullet}$, V_0^{x}	$V_0^{\bullet\bullet}$, V_0^{x}	$V_0^{\bullet\bullet}$, V_0^{x}
polyatomic paramagnetic	$Pb_n(i)$, i is odd and $<2n$	$Sn_n(i)$, i is odd and $<2n$	$Bi_n(i)$, i is odd for even n or even for odd n	$Ag_n(i)$, i is odd for even n or even for odd n
polyatomic diamagnetic and $\leq 2n$	$Pb_n(i)$, i is even and $\leq 2n$	$Sn_n(i)$, i is even and $\leq 2n$	$Bi_n(i)$ i is odd for odd n and even for even n	$Ag_n(i)$ i is odd for odd n and even for even n

Table II. Optical Spectroscopy Data (nanometers) for Pb(II)-β''-Alumina

observed band positions for colored Pb(II)-β''-alumina at 77 K	band positions for Pb(0) in KCl at room temp[17]	band positions for Pb$_2$ in argon at 10 K[23]
356, 440 (partially resolved)	339	
		434
	467	
508, 650		500
		606

Table III. Optical Spectroscopy Data (nanometers) for Sn(II)-β''-Alumina

obsd band positions in colored S(II)-β''-alumina at room temp	band positions for Sn(I) in KCl at 77 K[19]	band positions for Sn(0) in KCl at 85 K[18]	band positions, for Sn$_2$ in argon at 10 K[24]
410 (partially resolved)	200–225		
		470	
550			500
650 (partially resolved)			600

Table IV. Optical Spectroscopy Data (nanometers) for Bi(III)-β''-Alumina

obsd band position in colored Bi(III)-Na(I)-β''-alumina at room temp	band positions for Bi(I) in KCl at room temp[16]	band positions for Bi$_2$ in argon at 10 K[25]	band positions for Bi$_4$ in solid neon[26]
	305		
513		513	
		565	
653			778

Table V. Optical Spectroscopy Data for Ag(I)-β''-Alumina

obsd band positions in colored Ag(I)-β''-Alumina at room temp	obsd band positions for colored Ag–zeolite A at 243 °C assigned to Ag$_6$ cluster (reflectance spectra)[14]
317	
360	364
524	513
650	

dehydration reaction. Although the existence of F centers and certain monoatomic reduced cation species cannot be ruled out, the absorption bands from these species certainly do not account for the principal features of the observed optical absorption spectra.

Decomposition of Pb(II)-β''-Alumina by Hydrogen Reduction. The apparent existence of diatomic metal molecules in the β''-aluminas suggested that a second phase of colloidal metal might be formed under strongly reducing conditions. To see if this is true, a single crystal of Pb-(II)-β''-alumina was heated in 15% H$_2$/85% Na$_2$ gas at 750 °C for 1 h. The crystal became deeply colored. It was then pulverized, and the powder X-ray diffraction pattern examined. Every peak in the pattern could be assigned to Pb(II)-β''-alumina; no second phase could be detected. Next, a pulverized sample of Pb(II)-β''-alumina was heated in 15% H$_2$/85% N$_2$ gas at 650 °C for 1 h. Afterward, its powder diffraction pattern included new lines, indicating that new phases, had formed. A third sample, heated in 15% H$_2$/85% N$_2$ gas at 750 °C for 1 h revealed an even higher concentration of the new phases.

The powder diffraction patterns of the decomposed samples showed 11 new peaks, produced by two new phases. Four of the peaks were identified as the four most intense powder lines for metallic lead. The other seven peaks were indexed as a collapsed Pb(II)-β''-alumina structure in which every other conduction layer was missing. The approximate lattice parameters for such a structure are $a = 5.6$ Å and $c = 20.3$ Å. A similar structure was previously observed by Thomas et al. as an end product of the decomposition of NH$_4^+$/H$_3$O$^+$-β''-alumina.[28] It was also observed by Yang et al. as a product in the high-temperature decomposition of several β''-aluminas in oxidizing atmospheres.[29] The formation of Pb$_2$ dimers in large single crystals treated in hydrogen gas can be viewed as an intermediate step toward the formation of a second phase of lead metal. It is undoubtedly the much larger surface to bulk ratio of the pulverized samples that results in the precipitation of lead metal under similar reaction conditions.

Conclusions

This work has shown that several multivalent β''-aluminas can undergo redox reactions in which conduction layer cations are reduced to metal clusters during vacuum dehydration. These reduced species can later be oxidized back to their original state by a high-temperature treatment in the presence of oxygen. As a result of the vacuum dehydration reaction, these solid electrolytes, which normally are electronic insulators, become semiconductors. Their electronic conductivity is lower than their ionic conductivity. Although the reaction is reversible for large single-crystal samples, under extreme conditions, powdered samples of Pb(II)-β''-alumina have been shown to decompose into a pure metal phase and a collapsed structure. The formation of color centers during heating in inert atmosphere can be avoided by careful drying at elevated temperatures in oxygen.

(28) Thomas, J. O.; Eriksson, A.; Kjems, J.; Petford, A. *Solid State Ionics* **1986**, *18, 19*, 612.
(29) Yang, D. L.; Dunn, B.; Morgan, P. E. D., in press.